REPORT DOCUMENTATION PAGE

Form Approved
OMB No. 0704-0188

1. REPORT DATE *(DD-MM-YYYY)*	**2. REPORT TYPE**	**3. DATES COVERED** *(From - To)*
29-09-2014	Journal Article	May 2009 – April 2014

4. TITLE AND SUBTITLE
The Dynamic Characteristics of Silver Nanoparticles in Physiological Fluids: Toxicological Implications

5a. CONTRACT NUMBER

5b. GRANT NUMBER

5c. PROGRAM ELEMENT NUMBER

6. AUTHOR(S)
Laura Stolle1, Emily Breitner1, Kristen K. Comfort2, John J. Schlager1, and Saber M. Hussain1*

5d. PROJECT NUMBER
OAFW

5e. TASK NUMBER
P0

5f. WORK UNIT NUMBER
04/H04T

7. PERFORMING ORGANIZATION NAME(S) AND ADDRESS(ES)
1 *Molecular Bioeffects Branch, Bioeffects Division, Human Effectiveness Directorate, Human Performance Wing, Air Force Research Laboratory, Wright-Patterson AFB, Dayton, OH*
2 Department of Chemical and Materials Engineering, University of Dayton, Dayton, OH

8. PERFORMING ORGANIZATION REPORT NUMBER

9. SPONSORING/MONITORING AGENCY NAME(S) AND ADDRESS(ES)
Air Force Materiel Command
Molecular Bioeffects Branch
Bioeffects Division
Human Effectiveness Directorate
711th Human Performance Wing
Air Force Research Laboratory
Wright-Patterson AFB OH 45433-5707

10. SPONSOR/MONITOR'S ACRONYM(S)
711 HPW/RHDJ

11. SPONSORING/MONITORING AGENCY REPORT NUMBER
AFRL-RH-WP-JA-2014-0069

12. DISTRIBUTION AVAILABILITY STATEMENT Distribution A: Approved for public release; distribution unlimited. PA Case No. 88 ABW-2014-4133; date cleared 29 Aug 2014)

13. SUPPLEMENTARY NOTES

14. ABSTRACT
The field of nanotoxicology has made tremendous progress identifying novel and potentially adverse biological effects observed following nanomaterial (NM) exposure. However, one facet yet to be satisfactorily explored is how a physiological environment modifies NM physicochemical properties, thus introducing new and dynamic complexities involving solid phase material exposures. In this study, artificial alveolar, lysosomal, and interstitial fluids were used to mimic physiological environments for identifying material property aspects for hydrocarbon (Ag-HC) and polysaccharide (Ag-PS) coated silver NM. As inhalation is a common route of exposure, an alveolar macrophage cell model with deposition dosages representing approximately 2.5 months and 10 years of occupational exposure (0.5 and 25 ng/mL, respectively) were employed. Following dispersion in the artificial fluids, the Ag-HC and Ag-PS NPs demonstrated significant alterations to morphology, aggregation patterns, and particle reactivity. However, the Ag-PS also demonstrated a loss of particle coating, elicited an induced cytotoxicity, increased phagocytosis, and inflammation not associated with the original Ag-PS. This study demonstrated that in a physiological system NMs undergo considerable modulation introducing a scenario where NMs that were initially not to have frank toxicity do change over time with internal bioconditions. The dynamics of solid phase chemical material after exposure dosing remains a critical research area for defining the full bioeffects impact of nanomaterials with limited aqueous solubility.

15. SUBJECT TERMS
Artificial Fluids; Surface Coating; Ionic Dissociation; Immune Response

16. SECURITY CLASSIFICATION OF:			**17. LIMITATION OF ABSTRACT**	**18. NUMBER OF PAGES**	**19a. NAME OF RESPONSIBLE PERSON**
U					S. Hussain
a. REPORT	**b. ABSTRACT**	**c. THIS PAGE**	SAR	8	**19b. TELEPONE NUMBER (*Include area code)***
U	U	U			NA

Standard Form 298 (Rev. 8-98)
Prescribed by ANSI-Std Z39-18

Langmuir

Article

pubs.acs.org/Langmuir

Dynamic Characteristics of Silver Nanoparticles in Physiological Fluids: Toxicological Implications

Laura K. Braydich-Stolle,*[,†] Emily K. Breitner,[†] Kristen K. Comfort,[‡] John J. Schlager,[†] and Saber M. Hussain[†]

[†]Molecular Bioeffects Branch, Bioeffects Division, Human Effectiveness Directorate, Human Performance Wing, Air Force Research Laboratory, Wright-Patterson AFB, Dayton, Ohio 45433, United States

[‡]Department of Chemical and Materials Engineering, University of Dayton, Dayton, Ohio 45469, United States

Supporting Information

ABSTRACT: The field of nanotoxicology has made tremendous progress identifying novel and potentially adverse biological effects following nanomaterial (NM) exposure. However, one facet yet to be satisfactorily explored is how a physiological environment modifies NM physicochemical properties, thus introducing novel complexities associated with solid phase material exposures. In this study, artificial alveolar, lysosomal, and interstitial fluids were used to identify environmental-specific modulations to the properties and behavior of hydrocarbon-coated (Ag−HC) and polysaccharide-coated (Ag−PS) silver NMs. As inhalation is a common route of exposure, an alveolar macrophage cell model with deposition dosages representing approximately 2.5 months and 10 years of occupational exposure (0.5 and 25 ng/mL, respectively) were employed. Following dispersion in the artificial fluids, the Ag−HC and Ag−PS NMs demonstrated significant alterations to morphology, aggregation patterns, and particle reactivity. However, the Ag−PS also demonstrated a loss of particle coating, which elicited increased cytotoxicity, phagocytosis, and inflammation not associated with the original Ag−PS. This study demonstrated that in a physiological system NMs undergo considerable modulation, introducing a scenario where the toxicity of NMs may increase over time due to internal bioconditions. These findings highlight the critical influence that the dynamic and insoluble nature of NMs have on bioeffects and the importance of characterizing this behavior.

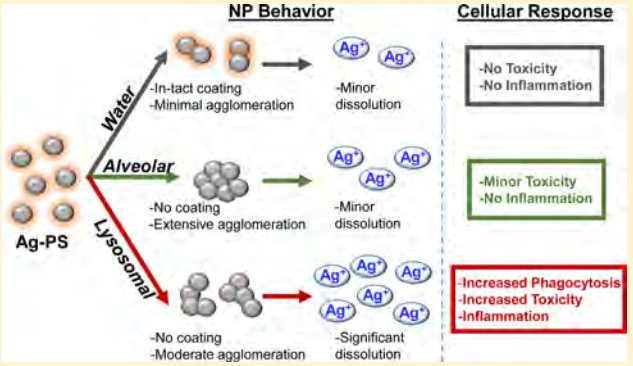

INTRODUCTION

The field of nanotoxicology has made significant progress in elucidating the impact of nanomaterials (NMs) on intracellular, organ, and whole organism biological systems. While the majority of studies have focused on final NM fate and resultant cellular damage, limited information is available on what role the immediate physiological environment plays in modifying the unique physicochemical properties of the NMs. Currently, silver nanoparticles (Ag NPs) incur the highest rates of utilization and exposure, due to their widespread use as an antimicrobial agent, with specific examples including bandages, surface coatings, clothing, and paint additives.[1−4] Extensive research has demonstrated a size- and dose-dependent cytotoxic effect of Ag NPs, with the mechanism of toxicity dependent on increased cellular stress and DNA damage.[5,6] Furthermore, due to the strong affinity between Ag and thiol groups,[7] Ag NPs robustly bind proteins and are capable of disrupting cellular functionality, even at subtoxic concentrations.[8−10] Many of the negative cellular consequences associated with Ag NP exposure have been mitigated by the addition of a surface coating that forms a boundary layer between the NP core and the cellular system.[8,11] However, surface modifications can be transient, suggesting that the cellular environment has the potential to alter NM characteristics and behavior as a function of time.

NMs behave differently from traditional chemical species in a biological environment, due to their insoluble nature and agglomeration tendencies.[12] For example, the transport mechanism for chemicals is comprised of direct diffusion and ion channels, whereas NMs are typically internalized through endocytosis.[13,14] The ability of NMs to agglomerate leads to atypical concentration gradients and greatly complicates dosimetry.[15] Moreover, through a dissolution process, NMs can disintegrate into ionic form over time, contributing to a prolonged effect. In recent years, ion effects have become a major focus of nanotoxicological research, with the general findings indicating that the dissolution of Ag NPs to ions is involved in the response but is not the sole cause of the observed cytotoxic and cellular consequences[16−20] In addition, these studies identified that the kinetic rate of ion production

Received: September 16, 2014
Revised: November 13, 2014
Published: November 19, 2014

   dx.doi.org/10.1021/la5036079 | Langmuir 2014, 30, 15309−15316

was dependent on a number of specific physicochemical properties, including primary size, temperature, environment, and surface chemistry. Specifically, ionic dissolution was highest with smaller and uncoated particles. Taken together, these situations highlight the complexities that arise following NM exposure and underscore the importance of identifying NM behavior in a physiological environment.

The three main routes of NM exposure are inhalation, ingestion, and absorption through the skin. Numerous in vitro studies have demonstrated the capability of NMs to pass through external biological membranes and enter a cell, typically through a combination of multiple endocytic mechanisms.[13,21] The endosomal vacuole containing NMs is believed to fuse with a lysosome, after which the particles will either remain within the lysosome or be released into the cytoplasm, where they interact with a number of major intracellular organelles.[22] In vivo exposure studies demonstrated that NMs easily penetrate small capillaries throughout the body, effectively distributing NMs throughout tissues, thus confirming their potential to pass through epithelia and impact any organ within the body.[23,24] Furthermore, in vivo studies have demonstrated that macrophages, immune cells that act as scavengers of foreign material, actively engulf and accumulate high concentrations of NMs following exposure. Therefore, while the exact fate and final location of NMs may not yet be fully understood, it is established that nanosized particles will encounter several biological fluids and environments post-exposure.

A major concern frequently overlooked is the free particle behavior and agglomeration kinetics of NMs in a physiological environment, which can influence outcomes such as cytotoxicity, internalization rate, and particle distribution.[19] However, due to the constraints associated with obtaining in vivo physiological samples, a significant knowledge gap exists pertaining to the environmental-specific influences on NM parameters and behavior. One potential solution to overcome this challenge is through the use of artificial fluids, which accurately mimic the composition and properties of a biological fluid.[25] A previous study by Stopford et al. examined the bioaccessibility of cobalt compounds in several artificial physiological fluids, including alveolar, lysosomal, and interstitial fluids,[26] which represent three of the most likely environments encountered by NMs.

The goal of this study was to demonstrate that the surrounding environment has the potential to alter NM behavior and ultimately influence toxicological effects. Due to their high inclusion rate in consumer products, known cytotoxic response, and high degree of ion production, Ag NPs were selected as a case study for this investigation. We examined the impact of artificial interstitial, alveolar, and lysosomal fluid on the physical properties of Ag NPs, the rate of ionic release, and the biological response over time in an alveolar macrophage cell line. This cell line was selected because of the considerations that inhalation is the most common NM exposure scenario and that macrophages actively seek and engulf NMs. Silver NMs are frequently in an aerosol form for applications such as antimicrobial sprays, disinfectants, and humidifiers,[27] further rationalizing the selection of an alveolar cell line. In vivo inhalation studies have reported conflicting results with regard to hazards associated with Ag NMs. In several instances, acute exposure resulted in no observable changes in lung function;[28,29] however, chronic exposure produced dose-dependent formation of lesions,[30] inflammatory responses,[30] decreased lung volume,[30] and DNA damage.[31] Moreover, due to the protective nature and influence of surface chemistry on Ag NP bioeffects, we evaluated fluid-specific influences on 25 nm Ag NPs with either a hydrocarbon or polysaccharide coating. Our data demonstrated that all the examined physical properties and the dependent biological responses of the Ag NPs were impacted following dispersion in physiologically relevant fluids. Furthermore, these modifications varied as a function of both initial surface chemistry and exposure duration, demonstrating the complex nature associated with NM behavior in an accurate biological system.

EXPERIMENTAL SECTION

Nanoparticles and Characterization. Hydrocarbon-coated silver (Ag−HC) nanoparticles with a 25 nm diameter were synthesized and generously received in powder form from Dr. Karl Martin of NovaCentrix, Austin, TX. For these nanoparticles, the surface hydrocarbon was not a continuous coating but rather an artifact of the manufacturing process that uses hydrocarbon to prevent sintering of the Ag nanoparticles during plasma synthesis. Polysaccharide-coated silver (Ag−PS) nanoparticles with a diameter of 25 nm were received dispersed in solution from Dr. Dan Goia's laboratory at Clarkson University, Potsdam, NY. For these Ag NPs, the coating was continuous and intentional with a thickness of 1−3 nm.

The size, morphology, and dispersion of the nanoparticles were characterized using transmission electron microscopy (TEM) and dynamic light scattering (DLS) using the methods previously described.[32] In addition, previous studies with these materials report extensive characterization of the NP surface chemistries.[8,11]

Composition of Artificial Fluids. Artificial alveolar, lysosomal, and interstitial fluids were made using the compositions reported by Stopford et al.,[26] which were formulated to accurately represent physiological conditions. Interstitial fluid is comprised of a number of salts and has a pH of 7.4. Alveolar fluid, also at pH 7.4, uses interstitial fluid as a base and is supplemented with the lipid phosphatidyl choline. Lysosomal fluid is a mixture of several salts, glycerin, and formaldehyde and has an acidic pH of 4.5. Table S1 of the Supporting Information shows the complete composition for each artificial fluid.

Nanoparticle Artificial Fluid Exposure. For the artificial fluid exposures, 10 mL of a 500 μg/mL solution was created for each Ag NP and fluid combination and incubated at 37 °C for 2, 6, 24, and 72 h. To ensure equal distribution and maintain particles in suspension, these water dispersed stocks were periodically vortexed. At the predetermined time the Ag NPs were separated from the fluid and ions using tangential flow filtration, as previously described by Maurer and co-workers.[20] The degree of ionic dissociation was evaluated in the supernatants using inductively coupled plasma mass spectrometry (ICP-MS). The recovered nanoparticles were resuspended in sterile water and the new concentration assessed using ICP-MS. The Ag NPs were then diluted to appropriate levels and recharacterized for TEM imaging and DLS. These recovered Ag NPs were then used in subsequent cellular assays.

Dosing Consideration for Exposure to Silver Nanoparticles. Various investigators in the field have experimentally evaluated the toxicity of NMs on the basis of a number of metrics, including particle number, mass, and surface area, as reviewed by Teeguarden et al.[33] Owing to the study design that included particle separation tangential flow, the only feasible dosing metric available was a per mass basis. However, to provide a more realistic exposure and dosimetry scenario, we employed a formula that converts the average amount of Ag inhaled in a standard worker over an 8 h work day into a single administered dose, normalized by respiratory rate (20 000 mL/min), pulmonary deposition efficiency for a 25 nm particle (~35%), average human lung surface area (102.2 m^2), and the OSHA-reported TLV-TWA value for silver (0.01 mg/m^3). This equation, which was provided by Dr. Jenny R. Roberts from the CDC/NIOSH, is shown below.

particle deposition in a standard worker (75 kg, male)

$$= (\text{respiratory rate}) \times (\text{air to liquid volume conversion}) \times (\text{TLV-TWA}) \times (\text{exposure time}) \times (\text{particle lung deposition efficiency})$$

$$= (20\,000\ \text{mL/min}) \times (1 \times 10^{-6}\ \text{m}^3/\text{mL}) \times (0.01\ \text{mg/m}^3) \times (480\ \text{min/day}) \times 0.35$$

$$= 0.0336\ \text{mg deposited/work day}$$

If the surface area of the human lung (~100 m^2) was included, the amount of exposure becomes 0.034 ng/cm^2 day, which when incorporating the surface area and volume of a standard culture medium translates into an in vitro dosing concentration of 0.01 ng/mL for 1 day of exposure. On the basis of this value, we chose to use concentrations of 0.5 and 25 ng/mL to represent approximately 2.5 months and 10 years of occupational exposure, respectively. On the basis of the report that NMs were retained in the lungs and displayed hindered clearance,[34] it is anticipated and assumed that materials would accumulate over time following inhalation.

Cell Culture. An alveolar macrophage cell line was chosen, as they are the cells most likely to interact significantly with the nanoparticles following inhalation. The U937 cell line was purchased from ATCC (CRL-1593.2), grown in RPMI-1640 media supplemented with 1% Pen-Strep and 10% heat-inactivated fetal bovine serum, and maintained in a humidified incubator at 37 °C with 5% CO_2. Prior to NP exposures, the U937 cells were stimulated with 100 ng/mL of phorbol-12-myristate-13-acetate (PMA) for 48 h to induce differentiation into macrophages and plated a cell density of 50 000 cells/well.

Cell Viability. The U937 cells were treated with 0.5 or 25 ng/mL of the Ag NPs sets for 24 h, and then cell viability was assessed using the MTS assay from Promega, in accordance with the manufacturer's procedure. Each experiment had six individual trials and was performed in triplicate. The data are represented as the mean ± the standard error, with statistical significance ($p < 0.05$) determined through a two-way ANOVA analysis with a Bonferroni post-test.

Expression of CD68 and CSFR-1. The cells were treated with 25 ng/mL of the fluid-exposed Ag NPs and incubated for 4 h, after which the expression of CD68 was examined to evaluate phagocytosis, along with the colony stimulating factor membrane bound receptor (CSFR-1) as activation markers. The cells were fixed with 4% paraformaldehyde and immunostained with antibodies against CD68 and CSFR-1 (Santa Cruz Biotechnology). Following staining, the samples were imaged on the BD Pathway 435, and the intensity of expression was quantified using the BD Pathway software and previously established protocols.[22]

Inflammatory Response. The cells were treated with 25 ng/mL of the indicated Ag NPs preparation sets for 8 h, the media was removed, and the presence of IL-6 and TNF-α was quantified using the human ELISA kits from BIOSOURCE according to the manufacturer's protocols. The data are represented as the average of six individual trials, run in triplicate, ± the standard error. A two-way ANOVA was performed, followed by Bonferroni post-tests, and $p < 0.05$ indicated significance.

RESULTS

Silver Nanoparticle Characterization. In order to identify environmental-specific alterations to the Ag NPs, select physicochemical properties were evaluated both prior to and following a 24 h exposure to artificial alveolar and lysosomal fluids. Using TEM analysis, significant modifications to both the NP primary size and morphology were observed for both particle sets in all tested fluids (Figure 1). The water-dispersed Ag−HC and Ag−PS had a primary size of 27.2 ± 6.1 and 23.2 ± 6.3 nm, respectively, with predominantly spherical morphology. Moreover, the polysaccharide coating surrounds the original Ag−PS particles was visible, identifiable in TEM images as the white ring around the particle perimeter, a pattern where the composition was previously verified to be the polysaccharide using X-ray photoelectron spectroscopy (XPS) (Braydich-Stolle et al.[8])

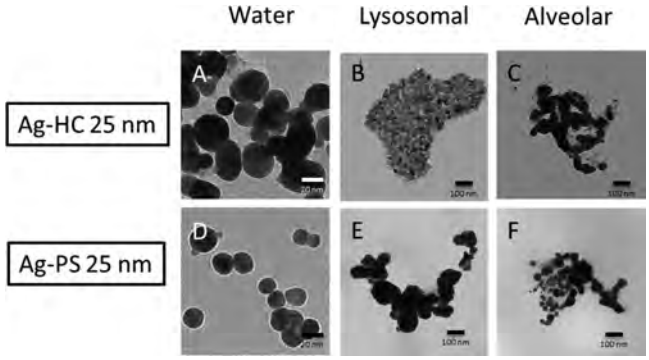

Figure 1. Silver nanoparticle morphology assessed using representative TEM images. Images are of (A) water Ag−HC, (B) lysosomal Ag−HC, (C) alveolar Ag−HC, (D) water Ag−PS, (E) alveolar Ag−PS, and(F) alveolar Ag−PS.

In lysosomal fluid, extensive fusing was seen with both coatings, as well as a complete loss of spherical morphology in the Ag−HC particles. Incubation in lysosomal fluid modified the primary particle size, as well as introducing a fused, or solid agglomerate, size. For Ag−HC particles, these sizes were 120.5 ± 35.8 and 290.1 ± 87.9 nm, respectively. For Ag−PS nanoparticles, the modified primary and fused diameters were also seen and were determined to be 50.3 ± 15.3 and 160.6 ± 50.1 nm. After a 24 h exposure to the alveolar fluid, both the Ag−HC and Ag−PS demonstrated significant aggregation and particle fusing when compared to the NP water images. Using TEM images, the individual and fused particles sizes were determined for both particle sets following incubation in alveolar fluid. This analysis showed single and agglomerate sizes of 68.5 ± 15.3 and 204.2 ± 68.6 nm for Ag−HC and 53.9 ± 8.8 and 341.1 ± 93.8 nm for Ag−PS, respectively. In addition, the distinctive coating previously seen with the Ag−PS water particles was not observed following dispersion in the artificial environments, indicating that the surface chemistry was altered during exposure to both alveolar and lysosomal fluids.

Previous studies have demonstrated that all NMs will agglomerate to some degree in solution,[32] with the extent of agglomeration impacting biobehavior and functionality. Using DLS, average aggregate sizes of the water dispersed solutions in water were determined to be 123.50 ± 4.50 and 52.10 ± 2.40 nm for the Ag−HC and Ag−PS respectively (Figure 2A). Following incubation in biological fluids, final aggregate size was re-evaluated and found to be significantly larger in a physiological environment (Figure 2A). The Ag−HC particles formed aggregates approximately 550 nm in size in both alveolar and lysosomal fluids. On the contrary, Ag−PS displayed a fluid specific aggregate pattern, with a significantly larger size associated with alveolar fluid (964.6 ± 18.0 nm) versus lysosomal fluid (218.7 ± 8.9 nm). This increase in DLS data is in excellent agreement with the TEM analysis that showed extensive particle fusing in the artificial fluids, with the largest fused size associated with Ag−PS incubation in alveolar fluid.

dx.doi.org/10.1021/la5036079 | Langmuir 2014, 30, 15309−15316

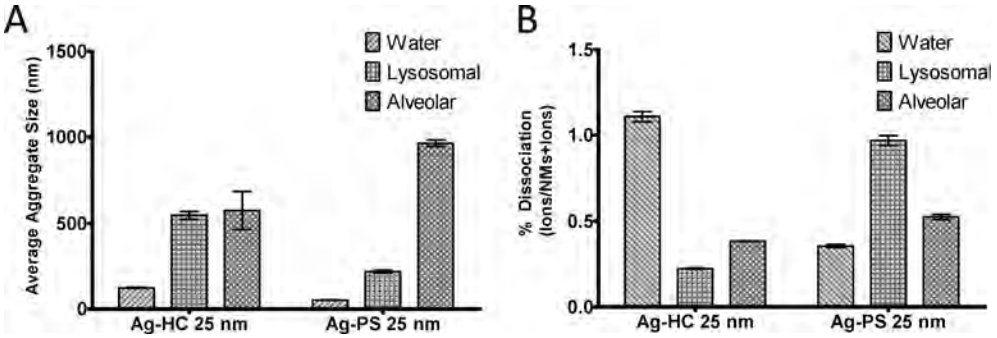

Figure 2. Influence of aqueous environment on silver nanoparticle characterization. (A) Effective aggregate size of silver particles as a function of environment. (B) Extent of ionic dissociation of silver particles after a 24 h duration.

Next, the level of silver ion (Ag^+) production from the NPs was evaluated using ICP-MS (Figure 2B). In water, the Ag−HC NPs were associated with a 1.1% ionic dissolution rate after 24 h. When placed in the different physiological environments, the ionic dissolution rate was reduced to 0.22% and 0.38% for lysosomal and alveolar fluid, respectively. In comparison, the water-dispersed Ag−PS demonstrated minimal Ag^+ production, only 0.35% after 24 h. The fact that the basal dissolution of Ag−PS is less than that of Ag−HC is likely due to the presence of the uniform particle coating, as surface chemistry has been shown to mitigate the rate of ion release.[27] An increase in the Ag−PS ion generation was found following exposure to physiological fluids, with lysosomal and alveolar fluids inducing 1% and 0.53% Ag^+ content, respectively. This increased rate of dissolution is in agreement with the TEM images that showed an elimination of the protective coating around the Ag−PS particles.

These characterization metrics were also carried out as a function of time, ranging from 0 to 72 h exposure durations. A time-dependent analysis of the Ag NP characterization indicated that that exposure duration did influence the particle physicochemical properties in lysosomal (Supporting Figure 1, Supporting Information) and alveolar fluids (Supporting Figure 2, Supporting Information). For lysosomal fluid, the aggregate size and dissolution rate of the Ag−HC particles stabilized quickly, whereas the Ag−PS displayed a dynamic nature. When dispersed in alveolar fluid, both particle sets showed stabilized dissolution around 24 h, while the extent of agglomeration continually increased with time.

Furthermore, we performed identical experimentation for the NPs in artificial interstitial fluid (Supporting Figure 3, Supporting Information), the most prevalent in vivo fluid, and found similar results to alveolar fluid exposure. Following dispersion in artificial interstitial fluid, the Ag NPs aggregate size continually increased over time, while the kinetic rate of ionic dissolution stabilized with time. However, for the sake of brevity and taking into account that inhalation is the most common form of NM exposure, the focus of this paper was on the 24 h exposure to alveolar and lysosomal fluids.

Silver Nanoparticle Toxicity. In order to determine if these fluid-specific alterations to Ag physical parameters had a direct impact on the macrophage cells, a cytotoxicity assessment was performed (Figure 3). After exposure to the 25 ng/mL dosage, both the water-dispersed and fluid-exposed Ag−HC particles induced negligible loss of cell viability. However, while the water-dispersed Ag−PS particles did not initiate a cytotoxic response, Ag−PSs modified by lysosomal and alveolar fluid exposure did produce a significant loss of viability. This

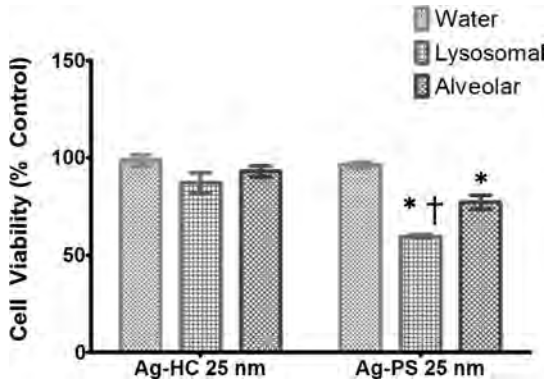

Figure 3. Changes in cell viability following 24 h exposure of Ag NPs. Ag NPs were incubated for 24 h in water, lysosomal fluid, or alveolar fluid, after which the particles were collected and dispersed in media at a concentration of 25 ng/mL. * denotes statistical significance from untreated controls; † denotes statistical significance from the water Ag NPs.

reduction in the number of viable macrophages, 39% and 23%, for lysosomal and alveolar fluids, respectively, are hypothesized to be due to the previously noted particle modifications, including loss of polysaccharide coating, increased ion dissolution, and the formation of large aggregates. Moreover, following exposure to interstitial fluid, no cytotoxicity was observed (Supplemental Figure 3, Supporting Information).

As one primary role of macrophages is to seek out and engulf foreign materials in an effort to protect the system, we explored if environmental modifications to the Ag NPs altered this response. We evaluated phagocytosis by measuring CD68 and CSFR-1 expression. The CD68 protein is a known marker for active phagocytosis, and CSFR-1 serves to normalize CD68 expression by ensuring equivalent cellular amounts.[35] In the Ag−PS lysosomal treatments, CD68 increased approximately 50% increase (Figure 4A,B), while the other treatments groups demonstrated comparable expression to control macrophages (Figure 4B and Supporting Figure 4, Supporting Information). For the CSFR-1 expression, there was no difference in expression for all of the treatment groups (Figure 4C); however, there was a difference in the localization of the protein (Figure 4A and Supporting Figure 4, Supporting Information). The CSFR-1 receptor is expressed at the surface of the cells and is not normally localized within the lysosomes of the cells. During phagocytosis, portions of the cellular membrane are ingested by the cell, and these membrane-enclosed vesicles ultimately fuse with the lysosomes. In the case of the Ag−PS lysosomal treatment, there is colocalization of

dx.doi.org/10.1021/la5036079 | Langmuir 2014, 30, 15309−15316

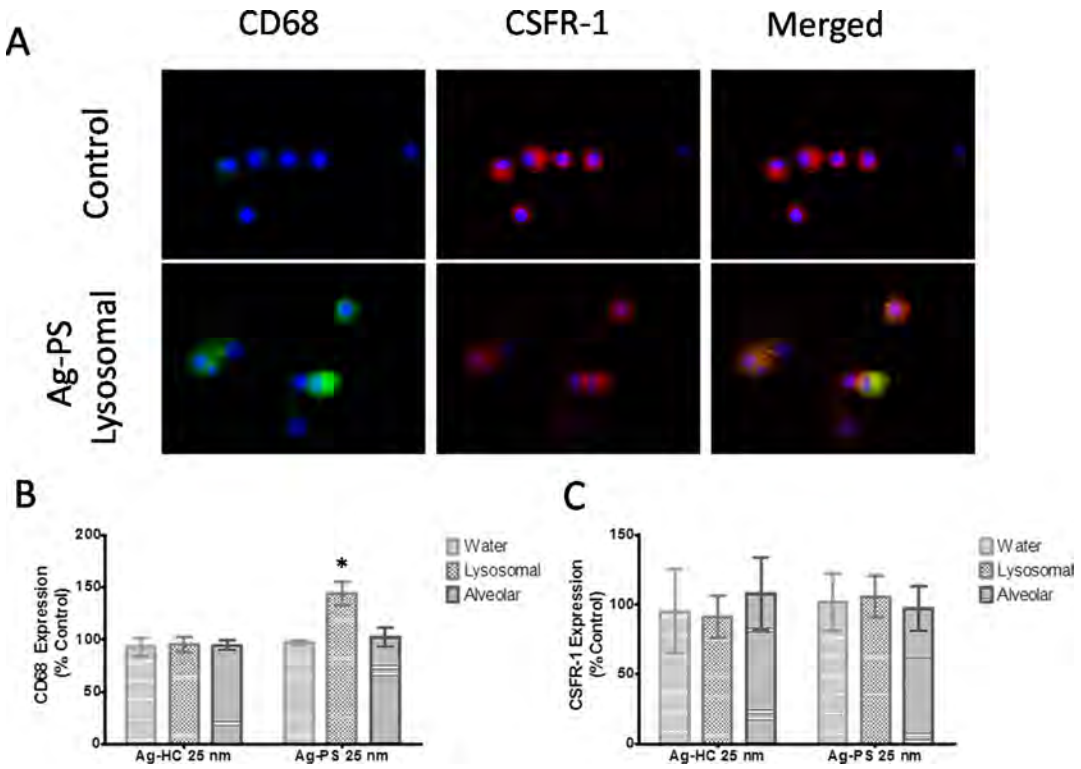

Figure 4. Expression of CD68 and CSFR-1 following treatment with Ag NPs exposed to artificial physiological fluids. (A) Representative confocal images that identify the expression and location of CD68 and CSFR-1. Quantification of (B) CD68 and (C) CSFR-1 expression as assessed from confocal images. * denotes statistical significance from untreated controls.

CSFR-1 and CD68, indicating that the membrane was being internalized by the cells and fused with the lysosome. Taken together, these results indicate that for the case of lysosomal exposed Ag–PS, an augmented degree of phagocytosis occurred.

In addition to phagocytosis, the secretion of pro-inflammatory cytokines IL-6 and TNF-α was evaluated for all Ag NP sets (Figure 5), as another function of macrophages is the secretion of cytokines to recruit additional cells to a sight of injury. For the macrophages exposed to the Ag–PS lysosomal fluid particles, IL-6 secretion increased 5-fold compared to the basal level in the untreated cells (Figure 5A). All other Ag NPs, including all Ag–HC sets and both water-dispersed and alveolar Ag–PS, demonstrated IL-6 secretion levels comparable to the untreated cells. A similar trend was observed with TNF-α secretion from differentiated U937 cells (Figure 5B). The increased production of IL-6 and TNF-α supports our previous results of increased cytotoxicity and phagocytosis, indicating that the cells are actively responding to the presence of these particles.

DISCUSSION

In order to investigate the impact of a physiological environment on NM physical characteristics and behavior, an experimental matrix was designed that consisted of 25 nm Ag NPs with two different surface coatings and three physiological environments. In addition to evaluating fluid-specific alterations to the physicochemical properties of NMs, this study investigated if these modulations produced new toxicological concerns. The physiological fluids employed in this study, alveolar, lysosomal, and interstitial, were selected on the basis of the prevalence and the probability of direct NM interaction.

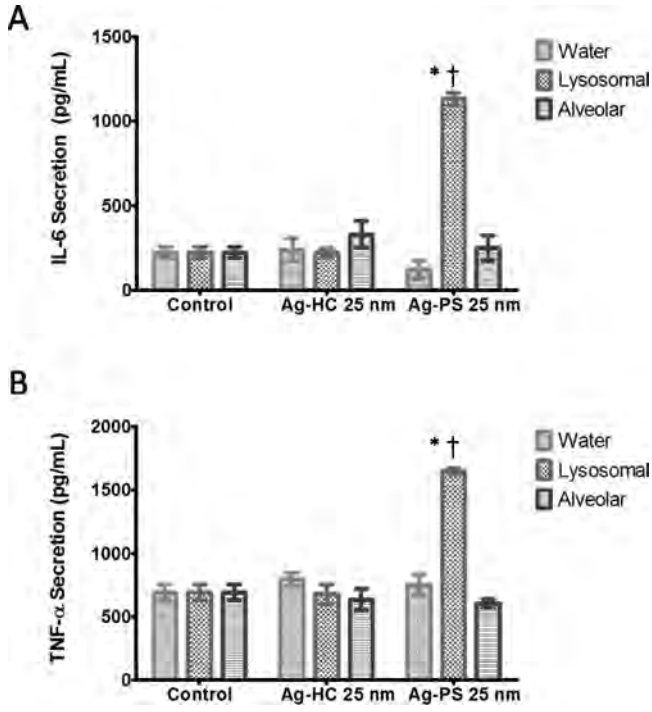

Figure 5. Secretion of inflammatory proteins following treatment with Ag NPs exposed to artificial physiological fluids. U937 cells underwent exposure to Ag NPs that were either water (stock) or lysosomal or alveolar fluid. After 24 h, the supernatants were evaluated for (A) IL-6 and (B) TNF-α production. * denotes statistical significance from untreated controls; † denotes statistical significance from the water Ag NPs.

dx.doi.org/10.1021/la5036079 | *Langmuir* 2014, 30, 15309–15316

Since inhalation is the most common form of NM exposure and NMs are known to penetrate deep into the alveolar region of the lungs, the examination of alveolar fluid was critical. Furthermore, NPs are known to be taken up via endocytosis both in vitro and in vivo by phagocytic cells, such as macrophages, highlighting the need to evaluate the influence of lysosomal fluid. We also chose to assess interstitial fluid, which surrounds cells and organ systems in the body, thus making it one of the most prevalent in vivo nonintracellular environments. Results indicated that Ag NP exposure to artificial fluids did significantly modify the innate characteristics and behavior of the particles; however, the degree of alteration was dependent on initial particle properties. Therefore, the discussion will focus on each particle set independently.

Hydrocarbon-Coated Silver Nanoparticles (Ag−HC). The hydrocarbon coating on these particles was formed as a byproduct during synthesis and was therefore nonuniform, making these particles very reactive by nature. When exposed to both alveolar and lysosomal fluid, the Ag−HC underwent extensive agglomeration and lost their distinctive spherical morphology, as determined through both DLS and TEM. This increase in agglomeration is in agreement with previous studies that have shown that NMs tend to aggregate in high ionic solutions, such as these artificial fluids.[36] The Ag−HC's incomplete coating caused high particle reactivity, resulting in a large percentage of ionic dissolution[37] in water, that was significant following exposure to the physiological fluids. We hypothesize this fluid-dependent decline in Ag^+ generation was brought on by a combination of two factors. First, because of the incomplete hydrocarbon coating, the water dispersed particles oxidized prior to fluid exposure.[38] Second, the rate of ion dissolution has been correlated to particle size, with greater production associated with smaller particles. Thus, due to the extensive particle agglomeration in the fluids, the surface area to volume ratio is significantly decreased, resulting in a lower particle reactivity rate.[39,40] These conclusions are in agreement with a previous report that claimed that Ag NPs in artificial fluid readily formed aggregates with minimal ionic dissolution.[41] Following introduction to the U937s, the Ag−HCs did not induce a cytotoxic response, alter rates of phagocytosis, or induce cytokine secretion, demonstrating that for this particle set bioresponses were not influenced by environmental alterations.

Polysaccharide-Coated Silver Nanoparticles (Ag−PS). The Ag−PS were purposefully coated with a 1−3 nm polysaccharide coating, thus minimizing agglomeration, reactivity, ionic dissociation (0.35%), and cytotoxicity in the water-dispersed solution. Similar to the Ag−HC, the Ag−PS underwent extensive agglomeration in both lysosomal and artificial fluids,[36] with a large fused particle size and an effective size of approximately 1000 nm associated with the alveolar fluid. During TEM evaluation, it was discovered that exposure to both alveolar and lysosomal fluids resulted in the elimination of the polysaccharide coating. From the time course evaluation, the loss of coating was seen within 2 h of exposure (Supplemental Figures 1A and 2B, Supporting Information). Previous research has demonstrated the tendency of polysaccharides to dissolve in ionic aqueous environment, supporting this observed coating loss.[42] In agreement with this finding, a previous study demonstrated that a 72 h exposure of the Ag−PS NPs to the lysosomal fluid resulted in a loss of coating and an increase in Ag content on the NP surface.[8] Furthermore, this modification to the surface chemistry was directly proportional to an increased rate of Ag+ production from Ag−PS NPs (Supplemental Figure 2C, Supporting Information). After 24 h, the ion production rate for Ag−PS NPs was determined as 0.53% in alveolar fluid and 1% in lysosomal fluid. This difference in ion production can be explained through the larger degree of agglomeration in alveolar fluid, which decreased the surface area to volume ratio, resulting in lower particle reactivity.[39,40]

Following incubation in the artificial fluids, the Ag−PS NPs were found to be toxic to the U937 cell line, though the degree of cytotoxicity was dependent on the fluid composition. Due to the extensive aggregation coupled with the lower reactivity, alveolar fluid exposed Ag−PS NPs were substantially less toxic than lysosomal treated particles, 23% vs 40%, respectively. Furthermore, a minimal degree of phagocytosis by macrophages and basal production of pro-inflammatory cytokines occurred with alveolar Ag−PS NPs, indicating that the biological response was not overtly damaging to its surrounding environment.

However, following introduction into a lysosomal solution, the Ag−PS displayed an extremely different response, both in terms of physical characteristics and induction of consequences in a cellular system. Owing to the loss of the PS coating and a lesser degree of aggregation, the Ag−PC displayed enhanced ionic dissolution following exposure to lysosomal fluid. Recent reports have identified that ionic dissolution is a contributor to metallic nanotoxicity,[17−20] partially explaining the observed cytotoxic response following exposure to these particles. Correlating with this observed loss of viability induced by the lysosomal-exposed Ag−PS NPs was the fact that this was the only particle set that displayed active phagocytosis and pro-inflammatory cytokine secretion. These results demonstrated that this specific subset of Ag NPs were interacting, being internalized, and initiating an inflammatory response within the U937 system, providing a second means of disrupting cellular homeostasis and inducing cytoxicity. A succinct summary of the Ag−PS behavior is presented in Figure 6.

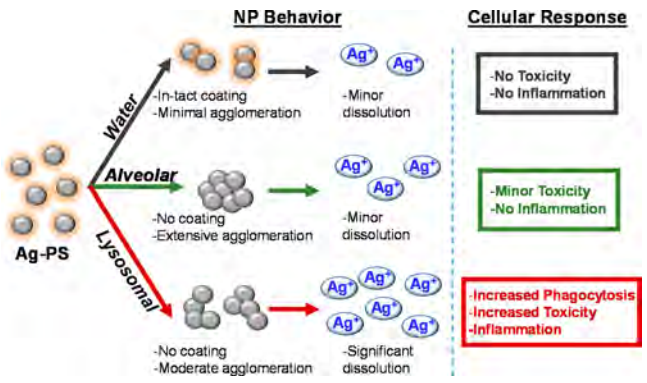

Figure 6. Summary of the results discovered during Ag−PS fluid exposure studies.

TNF-α acts in tandem with IL-6 to regulate a wide range of cell signaling pathways including NFκB production, apoptosis, and MAP kinase activity, which are mediated by reactive oxygen species (ROS) production.[43] The production of ROS has been shown to be a major player in the cell response to Ag nanomaterials. Therefore, the increased TNF-α and IL-6 production followed by a decrease in cell viability supports previous findings on Ag NP toxicity.[5,44−46] It is likely that the

dx.doi.org/10.1021/la5036079 | Langmuir 2014, 30, 15309−15316

unique characteristics associated with the lysosomal fluid exposed Ag−PS alter the nanocellular interface and initiate the significant degree of pro-inflammatory cytokine secretion.

CONCLUSIONS

Previous reports have focused on the direct effects that Ag NPs have on a biological system but have not investigated the impact of the physiological environment itself on the distinctive properties of the particles. In this study, we examined the behavior of two Ag−NPs, which at low dosages in their natural state did not initiate a cytotoxic or inflammatory response in an alveolar macrophage cell model. However, following exposure to artificial physiological fluids which mimic different cellular environments, these Ag NPs displayed changes in physical properties and behavior, demonstrating the ability of a biological environment to significantly impact distinctive NM parameters. We studied alveolar and lysosomal fluids, which represent the two most probable environments associated with inhalation as a route of exposure, correlating with our choice of an alveolar macrophage cell model. Our results indicated that both the original particle characteristics and the environmental composition played critical roles in the observed Ag NP responses, as Ag−HC remained nontoxic for all scenarios, but Ag−PS became cytotoxic following exposure to physiological fluids. Furthermore, this response was exacerbated with lysosomal fluid, owing to the dramatic physical alterations brought on by the acidic nature of this fluid (Figure 6). Therefore, this study has demonstrated the innate ability of a physiological system to significantly modulate NM physical properties and biological consequences, resulting in a new toxicological concern previously not identified. This research suggests that NM cellular internalization and subsequent contact with lysosomal fluid could transform nontoxic materials and initiate a novel cytotoxic response. Since NMs are insoluble and capable of accumulating in tissues and organs,[34] these findings suggest that NMs may amplify overall toxicity and inflammatory responses over time, presenting a scenario that must be further explored and addressed.

ASSOCIATED CONTENT

Supporting Information

Time course data for the lysosomal, alveolar, and interstitial fluid exposures and additional confocal images for all the treatment groups. This material is available free of charge via the Internet at http://pubs.acs.org.

AUTHOR INFORMATION

Corresponding Author

*Tel: 937-904-9495. Fax: 937-904-9610. E-mail: laura.stolle.ctr@us.af.mil.

Notes

The authors declare no competing financial interest.

ACKNOWLEDGMENTS

The authors would like to thank Mr. Brad Stacy for his assistance on the nanoparticle TEM imaging and Dr. Jenny Roberts for her assistance with dosing calculations. E.B. was funded under an ORISE fellowship and L.K.B.-S. is funded through the Henry Jackson Foundation.

REFERENCES

(1) Cioffi, N.; Ditaranto, N.; Torsi, L.; Picca, R.; De Giglio, E.; Sabbatini, L.; Novello, L.; Tantillo, G.; Bleve-Zacheo, T.; Zambonin, P. Synthesis, analytical characterization and bioactivity of Ag and Cu nanoparticles embedded in poly-vinyl-methyl-ketone films. *Anal. Bioanal. Chem.* **2005**, *382*, 1912−1918.

(2) Percival, S.; Bowler, P.; Dolman, J. Antimicrobial activity of silver-containing dressings on wound microorganisms using an in vitro biofilm model. *Int. Wound J.* **2007**, *4*, 186−191.

(3) Guggenbichler, J.; Samuel, U. J. Prevention of catheter-related infections: The potential of a new nano-silver impregnated catheter. *Int. J. Antimicrob. Agents* **2004**, *23*, S75−S78.

(4) Vigneshwaran, N.; Kathe, A.; Varadarajan, P.; Nachane, R.; Balasubramanya, R. Functional finishing of cotton fabrics using silver nanoparticles. *J. Nanosci. Nanotechnol.* **2007**, *7*, 1893−1897.

(5) Carlson, C.; Hussain, S.; Schrand, A.; Braydich-Stolle, L. K.; Hess, K.; Jones, R.; Schlager, J. Unique cellular interaction of silver nanoparticles: Size-dependent generation of reactive oxygen species. *J. Phys. Chem. B* **2008**, *112*, 13608−13619.

(6) AshaRani, P. V.; Mun, G. L.; Hande, M. P.; Valiyaveettil, S. Cytotoxicity and genotoxicity of silver nanoparticles in human cells. *ACS Nano* **2009**, *3*, 279−290.

(7) Hussain, S. M.; Meneghini, E.; Moosmayer, M.; Lacotte, D.; Anner, B. M. Potent and reversible interaction of silver with pure Na, K ATPase and Na, K ATPase liposomes. *Biochim. Biophys. Acta* **1994**, *1190*, 402−408.

(8) Braydich-Stolle, L. K.; Lucas, B.; Schrand, A.; Murdock, R. C.; Lee, T.; Schlager, J. J.; Hussain, S. M.; Hofmann, M. C. Silver nanoparticles disrupt GDNF/Fyn kinase signaling in spermatogonial stem cells. *Toxicol. Sci.* **2010**, *116*, 577−589.

(9) Comfort, K. K.; Maurer, E. I.; Braydich-Stolle, L. K.; Hussain, S. M. Interference of silver, gold, and iron oxide nanoparticles on epidermal growth factor signal transduction in epithelial cells. *ACS Nano* **2011**, *5*, 10000−10008.

(10) Comfort, K. K; Braydich-Stolle, L. K.; Maurer, E. I.; Hussain, S. M. Less is more: Long-term in vitro exposure to low levels of silver nanoparticles provides new insights for nanomaterial evaluation. *ACS Nano* **2014**, *8*, 3260−3271.

(11) Schrand, A. M.; Braydich-Stolle, L. K.; Schlager, J. J.; Dai, L.; Hussain, S. M. Can silver nanoparticles be useful as potential biological labels? *Nanotechnology* **2008**, *19*, 235104−235116.

(12) Oberdörster, G.; Oberdörster, E.; Oberdörster, J. Nanotoxicology: An emerging discipline evolving from studies of ultrafine particles. *Environ. Health Perspect.* **2005**, *113*, 823−839.

(13) Untener, E. A.; Comfort, K. K.; Maurer, E. I.; Grabinski, C. M; Comfort, D. A.; Hussain, S. M. Tannic acid coated gold nanorods demonstrate a distinctive form of endosomal uptake and unique distribution within cells. *ACS Appl. Mater. Interfaces* **2013**, *11*, 8366−8373.

(14) Yue, T.; Zhang, X. Cooperative effect in receptor-mediated endocytosis of multiple nanoparticles. *ACS Nano* **2012**, *6*, 3196−3205.

(15) Hirsch, V.; Kinnear, C.; Rodriquez-Lorenzo, L.; Monnier, CA; Rothen-Ruthishauser, B.; Baloq, S.; Petri-Fink, A. In vitro dosimetry of agglomerates. *Nanoscale* **2014**, *6*, 7325−7331.

(16) Navarro, E.; Piccapietra, F.; Wagner, B.; Marconi, F.; Kaegi, R.; Odzak, N.; Sigg, L.; Behra, R. Toxicity of silver nanoparticles to *Chlamydomonas reinhardtii*. *Environ. Sci. Technol.* **2008**, *42*, 8959−8964.

(17) Beer, C.; Foldbjerg, R.; Hayashi, Y.; Sutherland, D. S.; Autrup, H. Toxicity of silver nanoparticles—Nanoparticle or silver ion? *Toxicol. Lett.* **2012**, *208*, 286−292.

(18) Kim, J.; Kim, S.; Lee, S. Differentiation of the toxicities of silver nanoparticles and silver ions to the Japanese medaka (*Oryzias latipes*) and the cladoceran *Daphnia magna*. *Nanotoxicology* **2011**, *5*, 208−214.

(19) Zook, J. M.; Halter, M. D.; Cleveland, D.; Long, S. E. Disentangling the effects of polymer coatings on silver nanoparticle agglomeration, dissolution, and toxicity to determine mechanisms of nanotoxicity. *J. Nanopart. Res.* **2012**, *14*, 1−9.

(20) Maurer, E. I.; Sharma, M.; Schlager, J. J.; Hussain, S. M. Systematic analysis of silver nanoparticle ionic dissolution by tangential flow filtration: Toxicological implications. *Nanotoxicology* **2014**, *8*, 718−727.
(21) Iversen, T.; Skotland, T.; Sandvig, K. Endocytosis and intracellular transport of nanoparticles: Present knowledge and need for future studies. *Nano Today.* **2011**, *6*, 176−185.
(22) Braydich-Stolle, L. K.; Castle, A. B.; Maurer, E. I.; Hussain, S. M. Advantages of using imaged-based fluorescent analysis for nanomaterial studies. *Nanosci. Methods* **2013**, *1*, 137−151.
(23) Kashiwada, S. Distribution of nanoparticles in the see-through medaka (*Oryzias latipes*). *Environ. Health Perspect.* **2006**, *114*, 1697−1702.
(24) Almeida, J. P.; Chen, A. L.; Foster, A.; Drezek, R. In vivo biodistribution of nanoparticles. *Nanomedicine* **2011**, *6*, 815−835.
(25) Comfort, K. K.; Speltz, J. W.; Stacy, B. M.; Dosser, L. R.; Hussain, S. M. Physiological fluid specific agglomeration patterns diminish gold nanorod photothermal characteristics. *Adv. Nanopart.* **2013**, *2*, 336−343.
(26) Stopford, W.; Turner, J.; Cappellini, D.; Brock, T. Bioaccessibility testing of cobalt compounds. *J. Environ. Monit.* **2003**, *5*, 675−680.
(27) Reidy, B.; Haase, A.; Luch, A.; Dawson, K. A.; Lynch, I. Mechanisms of silver nanoparticle release, transformation and toxicity: A critical review of current knowledge and recommendations for future studies and applications. *Materials* **2013**, *6*, 2295−2350.
(28) Roberts, J. R.; McKinney, W.; Kan, H.; Krajnak, K.; Frazer, D. G.; Thomas, T. A.; Waugh, S.; Kenyon, A.; MacCuspie, R. I.; Hackley, V. A.; Castranova, V. Pulmonary and cardiovascular responses of rats to inhalation of silver nanoparticles. *J. Toxicol. Environ. Health A* **2013**, *76* (11), 651−68.
(29) Sung, J. H.; et al. Acute inhalation toxicity of silver nanoparticles. *Toxicol. Ind. Health* **2011**, *27*, 149−54.
(30) Sung, J. H.; et al. Lung function changes in Sprague−Dawley rats after prolonged inhalation exposure to silver nanoparticles. *Inhalation Toxicol.* **2008**, *20*, 567−574.
(31) Cho, H. S.; Sung, J. H.; Song, K. S.; Kim, J. S.; Ji, J. H.; Lee, J. H.; Ryu, H. R.; Ahn, K.; Yu, I. J. Genotoxicity of silver nanoparticles in lung cells of Sprague Dawley Rats after 12 weeks of inhalation exposure. *Toxics* **2013**, *1* (1), 36−45.
(32) Murdock, R.; Braydich-Stolle, L.; Schrand, A.; Schlager, J.; Hussain, S. Characterization of nanomaterial dispersion in solution prior to in vitro exposure using dynamic light scattering technique. *Toxicol. Sci.* **2008**, *101*, 239−253.
(33) Teeguarden, J. G.; Hinderliter, P. M.; Orr, G.; Thrall, B. D.; Pounds, J. G. Particokinetics in vitro: Dosimetry considerations for in vitro nanoparticle toxicity assessments. *Toxicol. Sci.* **2007**, *95*, 300−312.
(34) Möller, W.; Felten, K.; Sommerer, K.; Scheuch, G.; Meyer, G.; Meyer, P.; Haussinger, G.; Kreyling, W. Deposition, retention, and translocation of ultrafine particles from the central airways and lung periphery. *Am. J. Respir. Crit. Care Med.* **2008**, *177*, 426−432.
(35) Da Silva, R. P.; Gordon, S. Phagocytosis stimulates alternative glycosylation of macrosialin (mouse CD68), a macrophage-specific endosomal protein. *Biochem. J.* **1999**, *338*, 687−694.
(36) Gliga, A. R.; Skoglund, S.; Wallinder, I. O.; Fadeel, B.; Karlsson, H. L. Size-dependent cytotoxicity of silver nanoparticles in human lung cells: The role of cellular uptake, agglomeration and Ag release. *Part. Fibre Toxicol.* **2014**, *11*, 11.
(37) Li, Y.; Zhang, W.; Niu, J.; Chen, Y. Surface-coating-dependent dissolution, aggregation, and reactive oxygen species (ROS) generation of silver nanoparticles under different irradiation conditions. *Environ. Sci. Technol.* **2013**, *47*, 10293−10301.
(38) Lok, C. N.; Ho, C. M.; Chen, R.; He, Q. Y.; Yu, W. Y.; Sun, H.; Tam, P. K. H.; Chiu, J. F.; Che, C. M. Silver nanoparticles: Partial oxidation and antibacterial activities. *J. Biol. Inorg. Chem.* **2007**, *12*, 527−534.
(39) Zhang, W.; Yao, Y.; Sullivan, N.; Chen, Y. Modeling the primary size effects of citrate-coated silver nanoparticles on their ion release kinetics. *Environ. Sci. Technol.* **2011**, *45*, 4422−4428.
(40) Ma, R.; Levard, C.; Marinakos, S. M.; Cheng, Y.; Liu, J.; Michel, F. M.; Brown, G. E.; Lowry, G. V. Size-controlled dissolution of organic-coated silver nanoparticles. *Environ. Sci. Technol.* **2012**, *46*, 752−759.
(41) Stebounova, L. V.; Guio, E.; Grassian, V. H. Silver nanoparticles in simulated biological media: A study of aggregation, sedimentation, and dissolution. *J. Nanopart. Res.* **2009**, *13*, 233−244.
(42) Cumpstey, I. Chemical modification of polysaccharides. *ISRN Org. Chem.* **2013**, *2013*, 417672.
(43) Morgan, M. J.; Liu, Z. Crosstalk of reactive oxygen species and NF-κB signaling. *Cell Res.* **2011**, *21*, 103−115.
(44) Hussain, S. M.; Hess, K. L.; Gearhart, J. M.; Geiss, K. T.; Schlager, J. J. In vitro toxicity of nanoparticles in BRL 3A rat liver cells. *Toxicol. In Vitro* **2005**, *19*, 975−983.
(45) Braydich-Stolle, L.; Hussain, S.; Schlager, J. J.; Hofmann, M. C. In vitro cytotoxicity of nanoparticles in mammalian germline stem cells. *Toxicol. Sci.* **2005**, *88*, 412−419.
(46) Nel, A.; Xia, T.; Mädler, L.; Li, N. Toxic potential of materials at the nanolevel. *Science* **2006**, *311*, 622−627.